Power Laws in the Eigenvalue Distribution of MIMO Wireless Channels

Akbar M. Sayeed*and Vasanthan Raghavan
Department of Electrical and Computer Engineering
University of Wisconsin-Madison
akbar@engr.wisc.edu, vasanth@cae.wisc.edu
http://dune.ece.wisc.edu

Abstract

Power laws, a signature of scale-free behavior, are known to lurk behind many natural and man-made networks, including the metabolic system, Internet, World Wide Web, etc. Recent studies have identified two characteristics features in network evolution that are responsible for the existence of power laws: *incremental growth* and *preferential attachment* of new nodes to existing nodes in the network. In this paper we show empirical evidence that the ordered eigenvalues of a MIMO channel matrix exhibit a power law behavior characterized by two parameters. Based on physical principles, we argue that the two conditions for power law behavior are indeed satisfied in wireless channels. The power law induces an asymptotic density of eigenvalues that is not identical but quite similar to Silverstein's empirical eigenvalue density and yields consistent results on ergodic capacity. The relation with Silverstein's results is used to determine power law parameters. Power law behavior is also exhibited by certain correlated channels and is related to results in random banded matrix theory. This connection yields new insights on capacity scaling with the number of antennas in correlated channels.

1 Introduction

Recent studies, mostly based on empirical observations, show the existence of power laws underlying many man-made and natural networks, including the Internet, the human metabolic system, the World Wide Web (see, e.g. [1]). Typically, power laws indicate that the distribution of some variable of interest takes the functional form $y(x) \propto x^{\alpha}$. For example, the distribution of node connectivity (the number of nodes that a particular node is connected to) in the Internet exhibits a power law [1]. The existence of a power law indicates a "heavy tail" behavior in the distribution. For example, empirical studies show that the probability that a particular node in the Internet is connected to k other nodes decays as $k^{-\alpha}$ for some $\alpha > 0$ rather than the exponential decay predicted by earlier works based on random network models. Similarly, the eigenvalues of adjacency matrices in various networks have been shown to exhibit a power law behavior [1]. Recent works

*This research was supported in part by the National Science Foundation under grants CCR-9875805, ECS-9979408 and CCR-0113385, and the Office of Naval Research under grant N00014-01-1-0825.

by several researchers argue that the existence of power laws is related to the evolution of networks. In particular, two characteristic features in network evolution are responsible for the existence of power laws: *incremental growth* (the network grows by adding one node at a time) and *preferential (rather than random) attachment* of a new node to existing nodes in the network.

The behavior of multiple input multiple output (MIMO) channels encountered in wireless communication systems with antenna arrays is governed by the location of scattering objects encountered during propagation (see, e.g., [2, 3]). Realistic propagation environments correspond to multiple clusters of scattering objects. The MIMO channel corresponding to a system with N transmit and N receive antennas can be described as an $N \times N$ matrix. The recently introduced virtual MIMO channel representation [3] explicitly relates the scattering geometry to channel statistics and capacity. The virtual channel matrix is related to the actual channel matrix via a two-dimensional Fourier transfer. In particular, the $N \times N$ virtual channel matrix characterizes the scattering geometry in terms of N^2 virtual scatterers. Viewed this way, the MIMO channel can be construed as a network with the virtual scatterers acting as nodes. We argue using the virtual representation that MIMO channels satisfy the requirements of incremental growth and preferential attachment associated with the existence of power laws. First, as the number of antennas is increased, new virtual scatterers (nodes) contribute to the channel. Furthermore, the new virtual scatterers preferentially couple with the local virtual scatterers within the same scattering cluster.

In support of the above view of a MIMO wireless channel as a network of scattering nodes, we show empirical evidence that the eigenvalues of MIMO channels exhibit a power law behavior. Specifically, let the $N \times N$ matrix $\boldsymbol{H}$ denote the MIMO channel corresponding to N transmit and N receive antennas. The capacity of the MIMO channel is governed by the eigenvalues of $\boldsymbol{H}^H\boldsymbol{H}$. We show that the ordered eigenvalues of $\boldsymbol{H}^H\boldsymbol{H}$ can be closely approximated as

$$\lambda_i = Ai^{\alpha}, \quad i = 1, \cdots, N \tag{1}$$

where i is the index of *ordered* eigenvalues. Thus the eigenvalue distribution can be approximately characterized by the two parameters A and α. The power law (1) induces an asymptotic eigenvalue distribution that is not identical but close to the asymptotic empirical eigenvalue distribution obtained by Silverstein. This enables us to pin down the power law parameters. The power law behavior is also exhibited by correlated channels. We thus explore the asymptotic eigenvalue distribution of correlated channels using the power law framework in conjunction with the virtual channel representation and some results from random banded matrix theory (RBMT). In particular, we use an extension of Silverstein's asymptotic distribution suggested by RBMT that enables us to pin down the power law parameters in correlated channels. These results indicate that as long as the number of virtual scatterers grows at a fixed rate with the number of antennas, the only effect of correlation on asymptotic capacity is to reduce the SNR.

2 Power Laws

A quantity y as a function of some independent variable x is said to exhibit a power law if it takes the functional form

$$y(x) = Ax^{\alpha} \tag{2}$$

for some $A > 0$ and real-valued α. Taking the logarithm of (2) yields

$$\log[y(x)] = \log A + \alpha \log(x) \tag{3}$$

which states a characteristic feature of power laws: A log-log plot of the quantity follows a straight line with slope α and intercept $\log A$. The existence of power laws indicates a "heavy tail" distribution or *scale-free* behavior [1]. That is, there are no preferential scales in the distribution of the quantity. For example, the node connectivity distribution (number of nodes that a particular node is connected to) in the Internet follows a power law. This means that the probability that a node is connected to k other nodes decays as $k^{-\alpha}$, for some $\alpha > 0$. The power law distribution states that most nodes in the network are connected to very few nodes. However, for every scale of connectivity, there exist a few nodes exhibiting that level of connectivity. The power law behavior is intimately related to network topology: it suggests the existence of network "hubs" that are connected to a large number of other nodes, whereas most nodes are connected to few neighboring nodes. This is in contrast to the randomly connected network models used in the past. The existence of hubs and scale-free behavior is attributed to incremental growth and preferential attachment in network evolution.

The existence of power law behavior in the Internet is also related to the long range dependence observed in Internet traffic [4], which is in turn has led to fractal and multi-fractal based modeling of network traffic. The recently published book *Linked* [1] provides an excellent non-technical overview of the existence of power law behavior in a broad array of networks. It also includes references to some of the key recent works on this topic.

3 MIMO Wireless Channels

Consider a narrowband MIMO system consisting of a transmitter array with P elements and a receiver array with Q elements. In the absence of noise, the transmitted and received signals are related as

$$\boldsymbol{x} = \boldsymbol{H}\boldsymbol{s} \tag{4}$$

where $\boldsymbol{s}$ is the P-dimensional transmitted signal, $\boldsymbol{x}$ is the Q-dimensional received signal and $\boldsymbol{H}$ denotes the channel matrix coupling the transmitter and receiver elements. We index entries of $\boldsymbol{H}$ as $H(m,n):\ m = 0, 1, \cdots, Q-1,\ n = 0, 1, \cdots, P-1$.

For simplicity of exposition, we consider one-dimensional uniform linear arrays (ULAs) of antennas at both the transmitter and receiver and consider far-field scattering characteristics. Let d_T and d_R denote the antenna spacing at the transmitter and receiver, respectively. Then, the channel matrix can be described via the array steering and response vectors given by

$$\begin{aligned} \boldsymbol{a}_T(\theta_T) &= \frac{1}{\sqrt{P}}\left[1,\ e^{-j2\pi\theta_T}, \cdots, e^{-j2\pi(P-1)\theta_T}\right]^T \\ \boldsymbol{a}_R(\theta_R) &= \frac{1}{\sqrt{Q}}\left[1,\ e^{-j2\pi\theta_R}, \cdots, e^{-j2\pi(Q-1)\theta_R}\right]^T \end{aligned} \tag{5}$$

where θ and ϕ are related as

$$\theta = d\sin(\phi)/\lambda = \alpha\sin(\phi), \quad \phi = \sin^{-1}(\theta/\alpha), \tag{6}$$

λ is the wavelength of propagation, and $\alpha = d/\lambda$ is the normalized antenna spacing. The angle ϕ is measured relative to the horizontal axis (see Figure 1). The vector

$\boldsymbol{a}_R(\theta_R)$ represents the signal response at the receiver array due to a point source in the direction θ_R. Similarly, $\boldsymbol{a}_T(\theta_T)$ represents the array weights needed to transmit a beam focussed in the direction θ_T. We consider $\lambda/2$ antenna spacing in this paper resulting in $\alpha_T = \alpha_R = 1/2$.

3.1 Physical Modeling of Scattering Environment

For ULAs at the transmitter and receiver, the channel matrix $\boldsymbol{H}$ can be generally modeled as

$$\boldsymbol{H} = \int_{-1/2}^{1/2}\int_{-1/2}^{1/2} G(\theta_R,\theta_T)\boldsymbol{a}_R(\theta_R)\boldsymbol{a}_T^H(\theta_T)d\theta_R d\theta_T \tag{7}$$

$$H(m,n) = \frac{1}{\sqrt{PQ}}\int_{-1/2}^{1/2}\int_{-1/2}^{1/2} G(\theta_R,\theta_T)e^{-j2\pi\theta_R m}e^{j2\pi\theta_T n}d\theta_R d\theta_T, \tag{8}$$

where $G(\theta_R,\theta_T)$ represents the physical scattering and we call it the *spatial spreading function*. As evident from (8), $\boldsymbol{H}$ is a two-dimensional Fourier transform of $G(\theta_R,\theta_T)$. We note that in many realistic environments, $G(\theta_R,\theta_T)$ is non-vanishing in smaller regions corresponding to scattering clusters with limited angular spreads, as illustrated in Figure 1. Each cluster is represented by a non-vanishing sub-kernel of $G(\theta_R,\theta_T)$ with support $S_T \times S_R$, $S_T \subset [-1/2,1/2]$ and $S_R \subset [-1/2,1/2]$. A discrete path version of (7) is often used

$$\boldsymbol{H} = \sum_{l=1}^{L}\beta_l \boldsymbol{a}_R(\theta_{R,l})\boldsymbol{a}_T^H(\theta_{T,l}) \tag{9}$$

which describes the MIMO channel in terms of signal propagation over L paths with $\{\beta_l\}$ as the fading gains and $\{\theta_{R,l},\theta_{T,l}\}$ as the angles of arrival/departure associated with the paths. The discrete path physical model is illustrated in Figure 1(a).

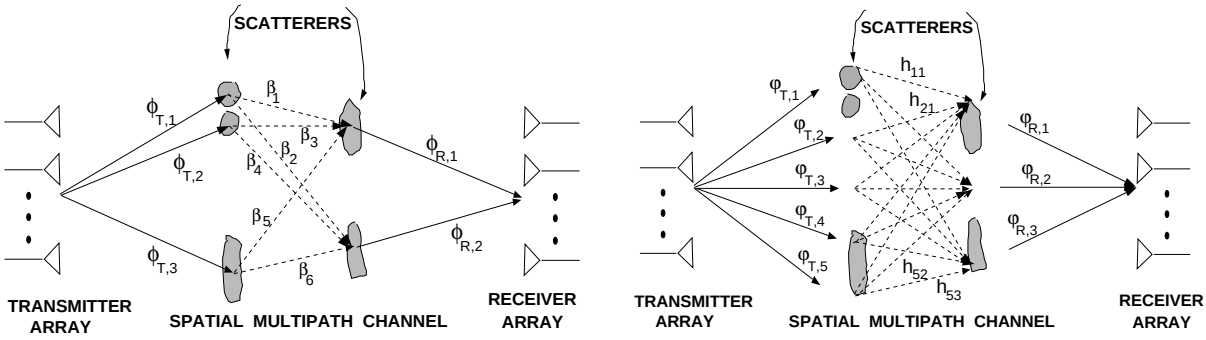

Figure 1: *A schematic illustrating* **physical channel modeling** *versus* **virtual channel representation**. *(a)* **Physical modeling.** *Each scattering path is associated with a fading gain (β_l) and a unique pair of transmit and receive angles ($\phi_{T,l}$, $\phi_{R,l}$) corresponding to scatterers distributed within the angular spreads. (b)* **Virtual representation.** *The virtual angles are fixed a priori and their spacing defines the spatial resolution. The channel is characterized by the virtual coefficients, $\{H_V(q,p) = h_{q,p}\}$, that couple the P virtual transmit angles, $\{\varphi_{T,p}\}$, with the Q virtual receive angles, $\{\varphi_{R,q}\}$.*

3.2 Virtual Channel Representation

The finite dimensionality of the spatial signal space can be exploited to develop a *linear* virtual channel representation which uses spatial beams in *fixed virtual* directions. Without loss of generality, we assume that both P and Q are odd and define: $\widetilde{Q} = (Q-1)/2$ and $\widetilde{P} = (P-1)/2$. The *virtual* channel representation, illustrated in Figure 1(b), can be expressed as [3]

$$\boldsymbol{H} = \sum_{q=-\widetilde{Q}}^{\widetilde{Q}} \sum_{p=-\widetilde{P}}^{\widetilde{P}} H_V(q,p)\boldsymbol{a}_R(\tilde{\theta}_{R,q})\boldsymbol{a}_T^H(\tilde{\theta}_{T,p}) = \widetilde{\boldsymbol{A}}_R \boldsymbol{H}_V \widetilde{\boldsymbol{A}}_T^H \tag{10}$$

where $\widetilde{\boldsymbol{A}}_R = [\boldsymbol{a}_R(\tilde{\theta}_{R,-\widetilde{Q}}), \cdots, \boldsymbol{a}_R(\tilde{\theta}_{R,\widetilde{Q}})]$ $(Q \times Q)$ and $\widetilde{\boldsymbol{A}}_T = [\boldsymbol{a}_T(\tilde{\theta}_{T,-\widetilde{P}}), \cdots, \boldsymbol{a}_T(\tilde{\theta}_{T,\widetilde{P}})]$ $(P \times P)$ are full-rank matrices defined by the fixed virtual angles $\{\tilde{\theta}_{R,q}\}$ and $\{\tilde{\theta}_{T,p}\}$. The virtual representation is *linear* and is characterized by the $Q \times P$ matrix $\boldsymbol{H}_V$ ($\widetilde{\boldsymbol{A}}_R$ and $\widetilde{\boldsymbol{A}}_T$ are fixed due to the fixed virtual angles). Uniform sampling of θ is a natural choice for virtual spatial angles which results in the steering/response vectors (5) being sinusoids with frequencies $\tilde{\theta}_{T,p}/\tilde{\theta}_{R,q}$, and yields *unitary* discrete Fourier transform (DFT) matrices $\widetilde{\boldsymbol{A}}_R$ and $\widetilde{\boldsymbol{A}}_T$. Since $\widetilde{\boldsymbol{A}}_R$ and $\widetilde{\boldsymbol{A}}_T$ are unitary, $\boldsymbol{H}_V$ is related to $\boldsymbol{H}$ $\boldsymbol{H}_V = \widetilde{\boldsymbol{A}}_R^H \boldsymbol{H} \widetilde{\boldsymbol{A}}_T$ and thus $\boldsymbol{H}_V$ is a two-dimensional DFT of $\boldsymbol{H}$ and captures all channel information. It can be shown that $\{H_V(q,p)\}$ are samples of a smoothed version of $G(\theta_R, \theta_T)$ at the virtual angles [3]. Specifically, we have the following sampling approximation for sufficiently large P and Q

$$H_V(q,p) \approx G(q/Q, p/P). \tag{11}$$

The sampling interpretation (11) has two important implications [3]. First, it provides an imaging interpretation of the scattering environment: different scattering clusters with limited angular spreads are represented by non-vanishing submatrices of $\boldsymbol{H}_V$. Second, under the reasonable assumption of spatially uncorrelated physical scattering, the non-vanishing elements of $\boldsymbol{H}_V$ are approximately uncorrelated. For ULAs this implies that the elements of $\boldsymbol{H}$ are a segment of a two-dimensional stationary random field and the elements of $\boldsymbol{H}_V$ are samples of the corresponding spectral representation.

Throughout this paper, we assume that $Q = P = N$. The elements of $\boldsymbol{H}_V$ are the coupling coefficients between different virtual scatterers (corresponding to fixed virtual angles). Thus, it can be viewed as describing the coupling between a network of virtual scatterers (nodes). The sampling relation (11) demonstrates that the properties of incremental growth and preferential attachment are satisfied in this network of virtual scatterers as the number of antennas increases. First, as N increases, more virtual scatterers couple with the channel due to the increased spatial resolution $\Delta\theta = 1/N$. Second, new virtual scatterers preferentially couple to other virtual scatterers within the same scattering cluster. The above conditions hold as long as there are sufficiently large number of physical propagation paths.

4 Power Laws in MIMO Channels

Viewing the MIMO wireless channel as a network of scatterers suggests the following question: Are there any power laws that govern the behavior of MIMO channels? Consider a MIMO channel described by the $N \times N$ matrix $\boldsymbol{H}$ consisting of iid Gaussian entries. It is well-known that the capacity of the channel is governed by the eigenvalues

of $\boldsymbol{H}^H\boldsymbol{H}$. Let $\lambda_i,\ i = 1, \cdots, N$ denote the eigenvalues of $\boldsymbol{H}^H\boldsymbol{H}$ in *increasing order*. Figure 2 shows log-log plots of the ordered eigenvalues as a function of the eigenvalue index for different values of N. Except for smaller indices, the plots indicate a remarkable linear behavior strongly indicating a power law distribution of the form (1).

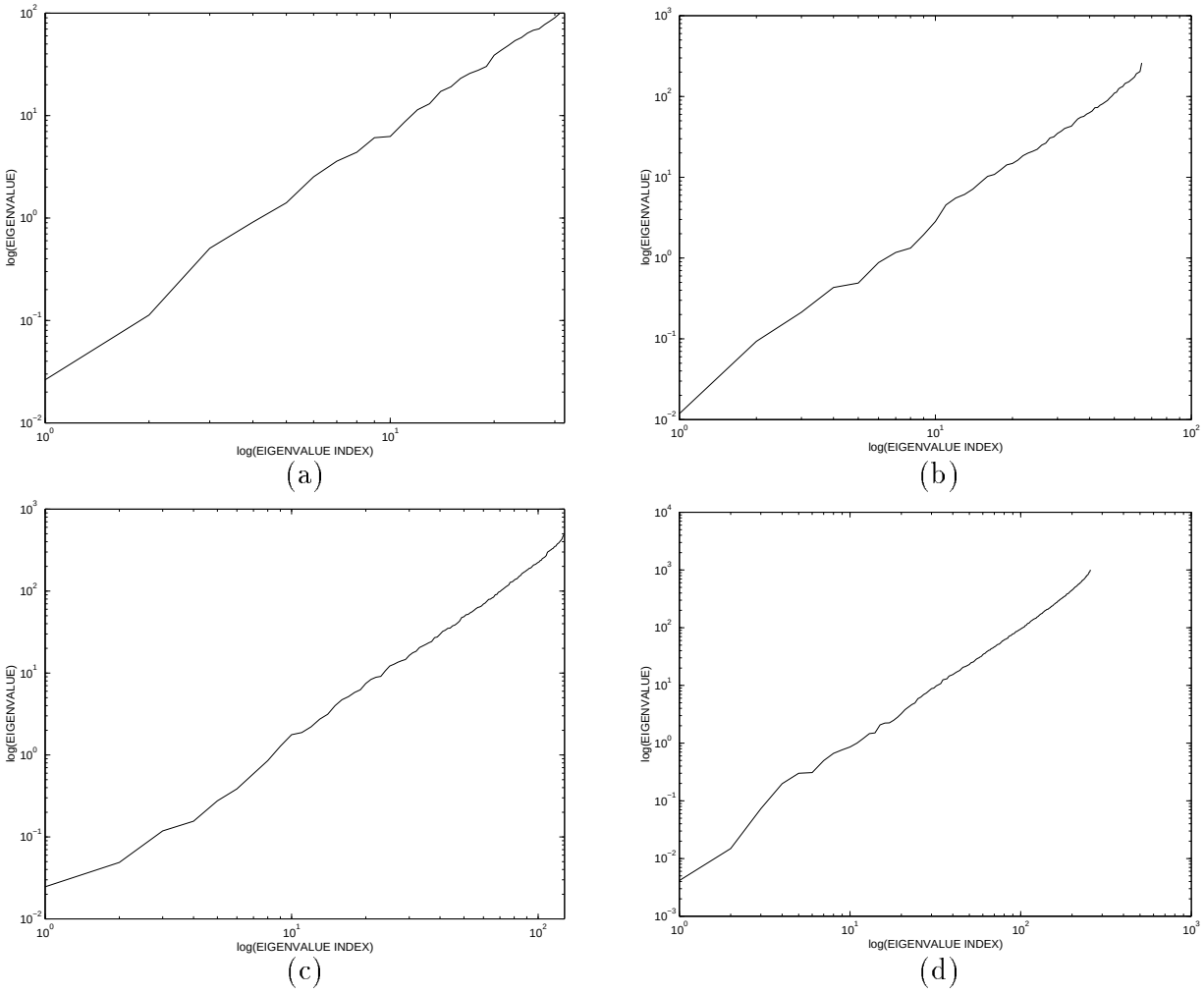

Figure 2: *Log-log plots of ordered eigenvalues of* $\boldsymbol{H}^H\boldsymbol{H}$ *for different values of* N. *(a) N=32. (b) N=64. (c) N=128. (d) N=256*

The power law (1) describes the N eigenvalues in terms of two parameters A and α. Clearly since the eigenvalues are random variables (due to randomness of $\boldsymbol{H}$), the values of A and α would also change with the channel realizations. Consider a noisy channel of the form

$$\boldsymbol{x} = \sqrt{\rho}\boldsymbol{H}\,\boldsymbol{s} + \boldsymbol{w} \tag{12}$$

where ρ denotes the SNR, $\mathrm{E}[\|\boldsymbol{s}\|^2] = 1$ and $\mathrm{E}[\boldsymbol{w}\boldsymbol{w}^H] = \boldsymbol{I}$. Conditioned on the knowledge of $\boldsymbol{H}$ at the receiver, the channel capacity is given by [5]

$$C(\boldsymbol{H}) = \log_2 \det(\boldsymbol{I} + \rho\boldsymbol{H}^H\boldsymbol{H}/N) = \sum_{i=1}^{N} \log_2(1 + \rho\lambda_i/N) \quad bits/sec/Hz. \tag{13}$$

The power law behavior suggests an alternative expression for capacity

$$C_{pl}(\boldsymbol{H}) \approx \sum_{i=1}^{N} \log_2(1 + \rho A i^{\alpha}/N) \quad bits/sec/Hz \tag{14}$$

that is characterized by the two parameters A and α. The ergodic capacity of the channel is then given by $C = \mathrm{E}[C(\boldsymbol{H})]$ where the expectation is over the ensemble of eigenvalues in (13) and its over the ensemble of A and α in (14).

Figure 3(a) plots the true ergodic capacity based on (13) as well as the ergodic capacity via the power law expression (14). The ergodic capacity is computed by ensemble averaging over 100 independent realizations of the channel. For computing C_{pl}, the parameters A and α are estimated for each channel realization using a least-squares fit. Figures 3(a) and (b) indicate that the ergodic capacities computed using (13) and (14) agree quite well. This suggests that the power law characterization of the eigenvalues is sufficiently rich to yield consistent values for ergodic capacity. The ensemble averaged values of α and $\log(A)$ are plotted in Figures 3(c) and (d). Note that α approaches an asymptotic value (≈ 2.2) whereas $\log(A)$ decreases with increasing N.

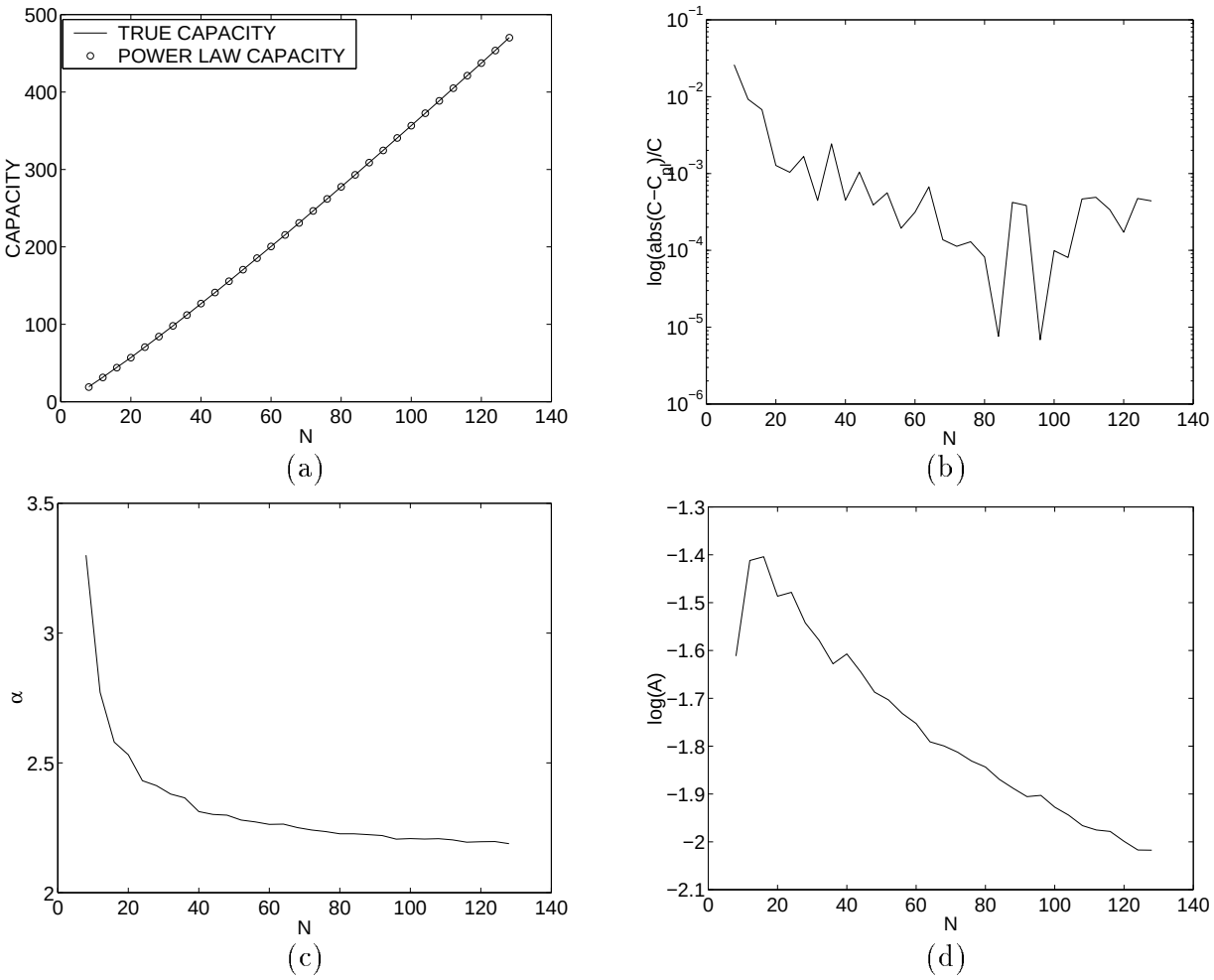

Figure 3: *Comparison of true ergodic capacity with that obtained via the power law characterization of eigenvalues. (a) Capacities as a function of N. (b) Log of the normalized error in capacity as a function of N. (c) Mean value of α as a function of N. (d) Mean value of $\log(A)$ as a function of N.*

5 Asymptotic Eigenvalue Density Induced by the Power Law

In the previous section, we estimated the parameters A and α by fitting the ordered channel eigenvalues to the power law curve. It is desirable to exploit some fundamental characteristics of the MIMO channel to determine A and α analytically. Basically, we need two constraints on the eigenvalues to determine the two unknowns A and α. One constraint is readily provided by the sum of the eigenvalues

$$\sum_{i=1}^{N} \lambda_i = A \sum_{i=1}^{N} i^{\alpha} \approx \text{trace}(\text{E}[\boldsymbol{H}^H \boldsymbol{H}]) = N^2 \tag{15}$$

where the approximation is due to the expectation on the right hand side and it gets better as N increases due to law of large numbers. For large N we also have the following approximation (Riemann sum approximation to the integral)

$$\frac{1}{\alpha+1} = \int_0^1 x^{\alpha} dx \approx \frac{1}{N} \sum_{i=1}^{N} (i/N)^{\alpha} = \frac{1}{N^{\alpha+1}} \sum_{i=1}^{N} i^{\alpha}. \tag{16}$$

Combining (15) and (16), we can eliminate the dependence of λ_i on A yielding

$$A \approx \frac{\alpha+1}{N^{\alpha-1}} \quad , \quad \lambda_i \approx \frac{\alpha+1}{N^{\alpha-1}} i^{\alpha} \ , i = 1, \cdots, N. \tag{17}$$

The value of α can be pinned down by examining the eigenvalue behavior for large N. In the limit of large N, (17) yields the following continuous power law characterization of the *normalized* ordered eigenvalue

$$\tilde{\lambda}_i = \lambda_i / N = (\alpha+1)(i/N)^{\alpha} \longrightarrow \tilde{\lambda}(x) = (\alpha+1)x^{\alpha}, \quad 0 \le x \le 1. \tag{18}$$

In particular, we have $\lambda_N / N = \lambda_{max} / N \longrightarrow \alpha + 1$. However, from earlier works on the asymptotic empirical eigenvalue distribution (see, e.g., Silverstein's work [6]) we know that $\lambda_N / N \to 4$ for iid channels. This suggests that $\alpha = 3$ for iid channels. However, empirical curve fitting suggests the value $\alpha \approx 2.2$. This suggests that the large eigenvalues are deviating from the power law behavior.

To further investigate the inconsistencies between theoretical and empirical values of α, we resort to comparing the asymptotic power law characterization of eigenvalues with that of Silverstein's. Silverstein derived the following expression for the asympototic probability density function (pdf) of the normalized eigenvalues

$$p_{\tilde{\lambda}}(\nu) = \frac{1}{\pi} \sqrt{1/\nu - 1/4}, \quad 0 \le \nu \le 4 \tag{19}$$

which implies that the largest normalized eigenvalue is 4 and the pdf goes to zero at $\nu = 4$. It also yields the following asymptotic expression for the normalized ergodic capacity

$$\frac{\text{E}[C(\boldsymbol{H})]}{N} \longrightarrow \frac{1}{\pi} \int_0^4 \log_2(1+\rho\nu) \sqrt{1/\nu - 1/4} d\nu. \tag{20}$$

In the power law expression (18) for asymptotic eigenvalue behavior, consider $\tilde{\lambda}(x)$ as a random variable defined on the probability space $\{x : 0 \le x \le 1\}$ with uniform measure. Then, the uniform measure on $\{x \in [0,1]\}$ induces the following pdf for $\tilde{\lambda}_x$

$$p_{\tilde{\lambda},pl}(\nu) = \frac{1}{\alpha} \frac{\nu^{(1-\alpha)/\alpha}}{(\alpha+1)^{1/\alpha}}, \quad 0 \le \nu \le \alpha + 1. \tag{21}$$

and a corresponding expression for the normalized capacity

$$\frac{\mathrm{E}[C_{pl}(\boldsymbol{H})]}{N} \longrightarrow \int_0^1 \log_2(1+\rho(\alpha+1)x^{\alpha})dx = \frac{1}{\alpha(\alpha+1)^{1/\alpha}} \int_0^{\alpha+1} \log_2(1+\rho\nu).\nu^{(1-\alpha)/\alpha}d\nu \tag{22}$$

Figure 4 compares the power-law density with that due to Silverstein. Note that while $p_{\tilde{\lambda}}(\nu)$ goes to zero at $\nu = 4$, $p_{\tilde{\lambda},pl}(\nu)$ goes to a non-vanishing value at $\nu = \alpha + 1$. It is evident that even the Silverstein density exhibits a strong power-law behavior (linear log-log plot) for values of ν away from the maximum. The log-log plot drops rapidly to $-\infty$ at $\nu = 4$ since the pdf goes to zero. The power law density for $\alpha = 2.2$ gives a very good fit to the Silverstein's density away from the maximum. We note that at at SNR of 20dB ($\rho = 100$), the Silverstein formula (20) yields (for large N) $C/N \approx 5.47$ whereas the power law capacity expression in (22) yields $C/N \approx 5.01, 5.47$ for $\alpha = 3, 2.2$, respectively.

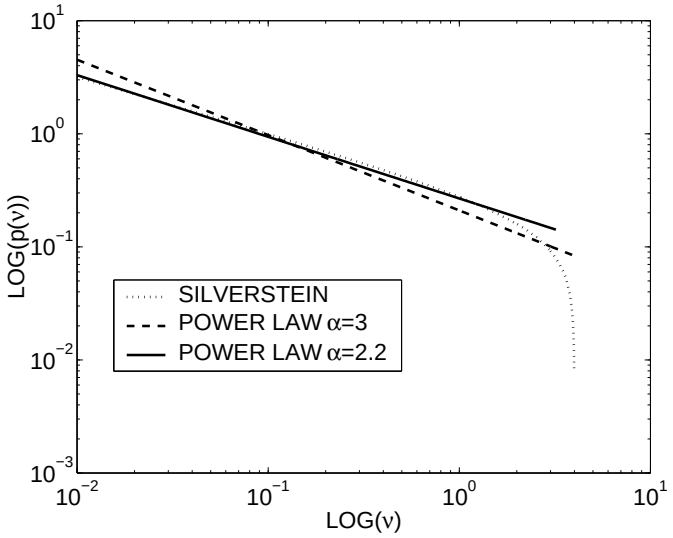

Figure 4: *Comparison of log-log plots of Silverstein's asymptotic eigenvalue density and power-law densities.*

6 Power Laws in Correlated Channels

Based on physical considerations, the virtual representation suggests a k-diagonal model for correlated channels [3]. The k-diagonal model corresponds to $\boldsymbol{H}_V$ consisting of k non-vanishing diagonals with iid entries. For example, k=1 corresponds to a diagonal channel (most correlated) and k=N corresponds to the iid model.

Suppose that $a = k/N$ remains fixed as N increases. Results in Random Banded Matrix Theory (RBMT) [7, 8] (and also some earlier work of Silverstein) suggest the following generalization of (20) for asymptotic capacity of such k-diagonal channels

$$\frac{\mathrm{E}[C(\boldsymbol{H})]}{N} \longrightarrow \frac{1}{\pi} \int_0^4 \log_2(1+a\rho\nu)\sqrt{1/\nu - 1/4}d\nu. \tag{23}$$

The above relation implies that as long as k scales linearly with N, the only effect of correlation (in the context of k-diagonal models) on asymptotic capacity is a reduction in SNR by the factor $a = k/N$.

Power law characterization of eigenvalues also applies to k-diagonal channels. The only difference is that we have a different trace constraint: $\mathrm{E}[\boldsymbol{H}^H\boldsymbol{H}] = N + 2N(k-1) - k(k-1)$. This yields a different value for the power law constant A. With this modification, the normalized capacity expression (22) based on the power law becomes

$$\begin{aligned}\frac{\mathrm{E}[C_{pl}(\boldsymbol{H})]}{N} &\longrightarrow \int_0^1 \log_2(1+\rho a(2-a)(\alpha+1)x^\alpha)dx \\ &= \frac{1}{\alpha[a(2-a)(\alpha+1)]^{1/\alpha}}\int_0^{a(2-a)(\alpha+1)} \log_2(1+\rho\nu)\nu^{(1-\alpha)/\alpha}d\nu. \quad (24)\end{aligned}$$

7 Conclusion

In this paper we have presented empirical evidence for the existence of power laws in the ordered eigenvalue distribution of MIMO channel matrices. For iid channels, the power law characterization yields a an asymptotic eigenvalue density that is quite similar to that obtained by Silverstein except at large values of normalized eigenvalues. The power law behavior is exhibited in the case of correlated channels as well and, in conjunction with results from RBMT theory, it suggests a new expression for normalized ergodic capacity of correlated channels. The results indicate that, under certain conditions, the only efect of correlation on asymptotic capacity is to reduce the effective SNR by a factor related to the degree of correlation. More detailed discussion of such capacity scaling in correlated channels will be reported elsewhere.

References

[1] A.-L. Barabási, *LINKED: The New Science of Networks.* Perseus Publishing, 2002.

[2] J. Fuhl, A. F. Molisch, and E. Bonek, "Unified channel model for mobile radio systems with smart antennas," *IEE Proc. Radar, Sonar Navig.*, vol. 145, pp. 32–41, Feb. 1998.

[3] A. M. Sayeed, "Deconstructing multi-antenna fading channels," *IEEE Trans. Signal Processing*, vol. 50, pp. 2563–2579, Oct. 2002.

[4] J. Beran, R. Sherman, M. Taqqu, and W. Willinger, "Long-range dependence in variable-bit-rate video traffic," *IEEE Trans. Commun.*, vol. 43, pp. 1566–1579, Feb./Mar./Apr. 1995.

[5] E. Telatar, "Capacity of multi-antenna gaussian channels," *AT& T-Bell Labs Internal Tech. Memo.*, June 1995.

[6] J. W. Silverstein and Z. D. Bai, "On the empirical distribution of eigenvalues of a class of large dimensional random matrices," *J. Mult. Var. Anal.*, vol. 54, no. 2, pp. 175–192, 1995.

[7] Y. V. Fyodorov, O. A. Chubykalo, F. M. Izrailev, and G. Casati, "Wigner random banded matrices with sparse structure: Local spectral density of states," *Phy. Rev. Letts.*, vol. 76, pp. 1603–1606, Mar. 1996.

[8] M. Kuś, M. Lewenstein, and F. Haake, "Density of eigenvalues of random banded matrices," *Phy. Rev. A*, vol. 44, pp. 2800–2808, Sep. 1991.